Expanded View Figures

Figure EV1. Mouse model and experimental design.

A Genetic model to study the GC reaction with a fluorescent tracer. AicdaCre$^{+/ki}$; R26tdTom$^{+/ki}$ (Aicda$^{Cre/+}$), and AicdaCre$^{-/ki}$; R26tdTom$^{+/ki}$ (Aicda$^{Cre/-}$) mice are shown.
B Complete gating strategy for B cell subsets analyzed in Fig 1B and C.
C FACS representative plots and quantification of IgG1, IgG2B, and IgG2C within B cell populations in Fig 1C (n = 6 Aicda$^{Cre/+}$ mice).
D Antibody titers specific for OVA were measured in the plasma of control Aicda$^{Cre/+}$ mice (PBS; n = 3) and immunized Aicda$^{Cre/+}$ mice (OVA; n = 8) by ELISA. Statistics were calculated with the paired t-test. ****$P < 0.0001$. n indicates biological replicates.
E Experimental approach followed for single cell RNA sequencing.

Data information: Bars and error bars indicate mean ± standard deviation.

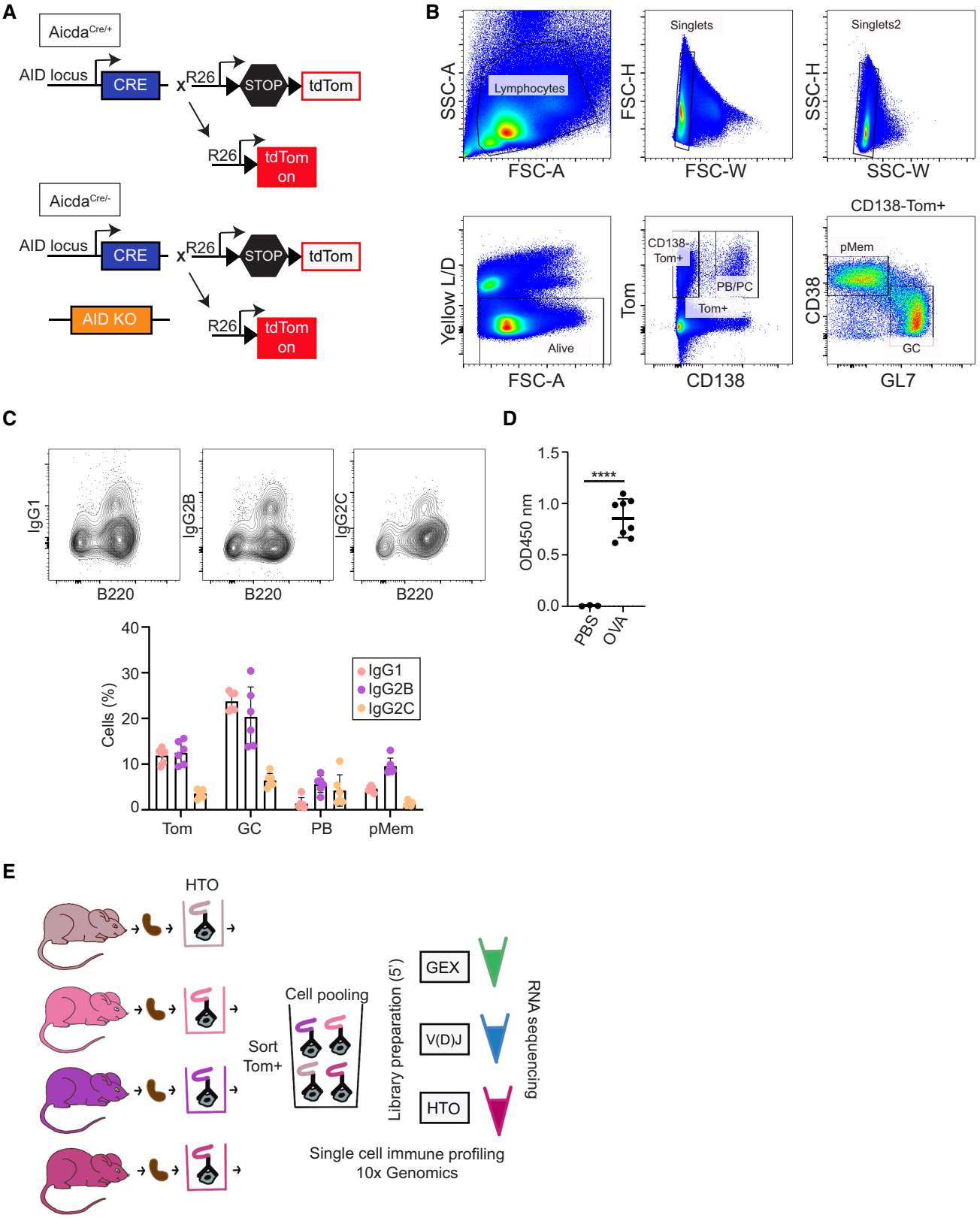

Figure EV1.

Figure EV2. Cluster analysis.

A UMAP plot showing transcriptional clusters obtained before cluster 0 subclustering.
B UMAP plot showing three transcriptionally distinct subclusters (0a, 0b, and 0c).
C Dot plot depicting the expression levels of the top 10 upregulated genes in clusters 0a, 0b, and 0c.
D Anti-FcRγ antibody test. Representative flow cytometry plots of B3Z (NIH) parental cells (left) and FcRγ-CD2-transfected cell lines stained with anti-FcRγ and anti-CD2 antibodies.
E Gating strategy for L-prePB identification by flow cytometry and cell sorting. L-prePB backgating shown in black.
F Expression analysis of the indicated genes obtained by scRNA-seq shown in Fig 3A. [a]Average log2 fold change between the two groups being compared. [b]Proportion of cells expressing the indicated gene within FcRγ$^+$ cells. [c]Proportion of cells expressing the indicated gene within the non-FcRγ$^+$ cells.
G FACS representative plot for L-prePB staining in the spleen of Aicda$^{Cre/+}$ mice 2 weeks after a single OVA immunization.
H Anti-FcRγ staining in GL7$^-$ and GL7$^+$ cells within live, singlets, Tom$^+$, CD138$^-$, B220$^+$ gated cells.
I Aicda$^{Cre/+}$ mice (n = 7) were immunized with OVA following the protocol in Fig 1A. Four mice were sacrificed 2 weeks after the first immunization. The proportion of prePB (Tom$^+$ B220$^+$ CD138$^-$ GL7$^-$ FcRγ$^+$) and PB (Tom$^+$ CD138$^+$) cells was determined by flow cytometry within total live cells.

Data information: Bars and error bars indicate mean ± standard deviation.

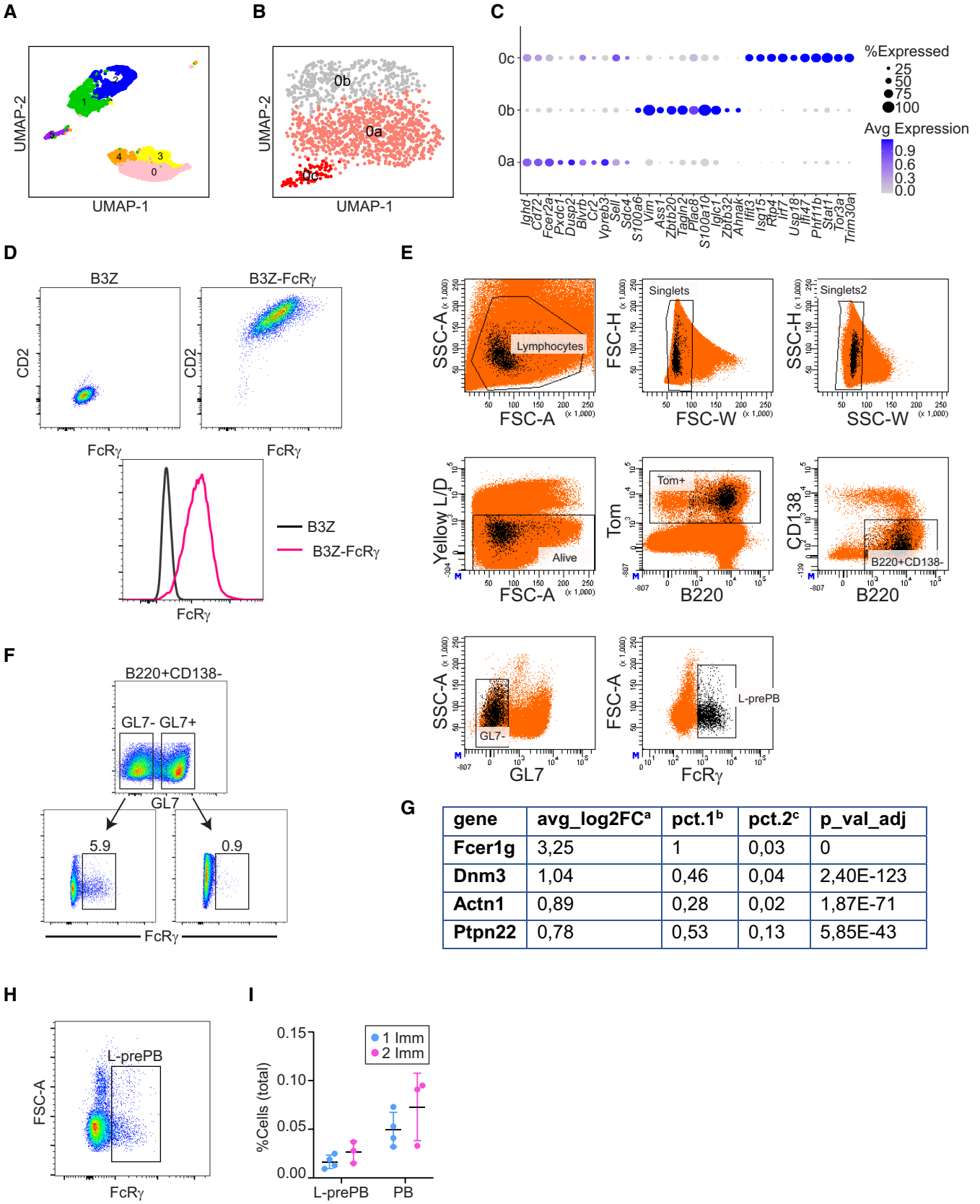

gene	avg_log2FC[a]	pct.1[b]	pct.2[c]	p_val_adj
Fcer1g	3,25	1	0,03	0
Dnm3	1,04	0,46	0,04	2,40E-123
Actn1	0,89	0,28	0,02	1,87E-71
Ptpn22	0,78	0,53	0,13	5,85E-43

Figure EV2.

A

	GC.LZ	E-prePB	Mem.Act	Mem.GC	Mem.Act2	L-prePB	PB
GC.DZ	0,2321	**<0,0001**	**<0,0001**	**<0,0001**	**<0,0001**	**<0,0001**	**<0,0001**
GC.LZ		**<0,0001**	**<0,0001**	**<0,0001**	**<0,0001**	**<0,0001**	**<0,0001**
E-prePB			0,5819	**<0,0001**	>0,9999	**0,0083**	0,1368
Mem.Act				**<0,0001**	>0,9999	**<0,0001**	**0,0001**
Mem.GC					**0,0003**	>0,9999	>0,9999
Mem.Act2						**0,0182**	**0,0394**
L-prePB							>0,9999

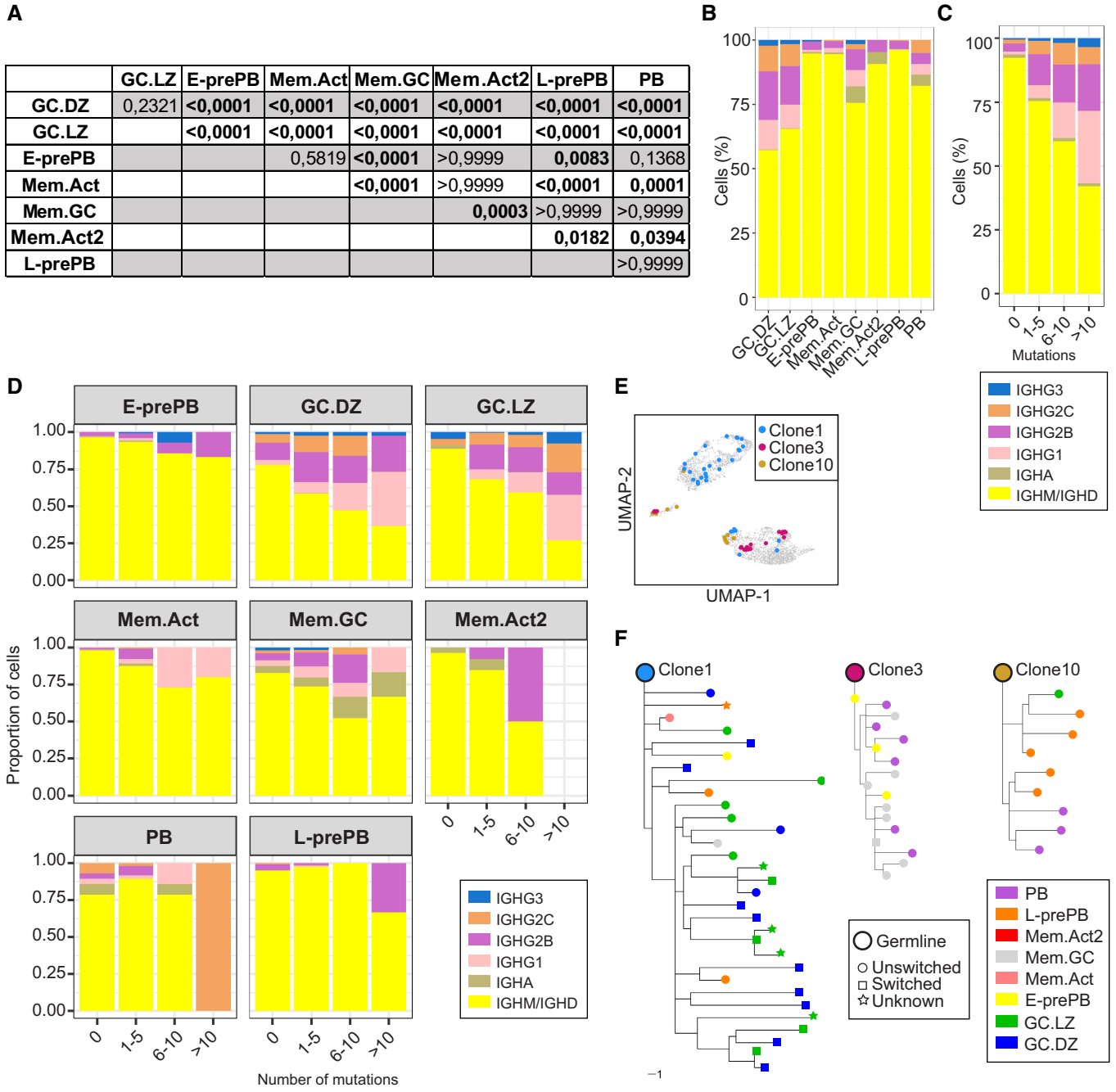

Figure EV3. SHM and CSR analysis.

A *P*-values for the SHM data shown in Fig 4A. Statistics were calculated with the Kruskal–Wallis test.
B Quantification of the different isotypes within B cell clusters.
C, D Isotype quantification in total B cells (C) and individual clusters (D) according to their different mutational load.
E UMAP plot showing 3 representative expanded clones (clone1, clone3, and clone10).
F Trees showing phylogenetic relationships between IgH sequences of clone1, clone3, and clone10 of panel E. Scale bar: 1 mutation.

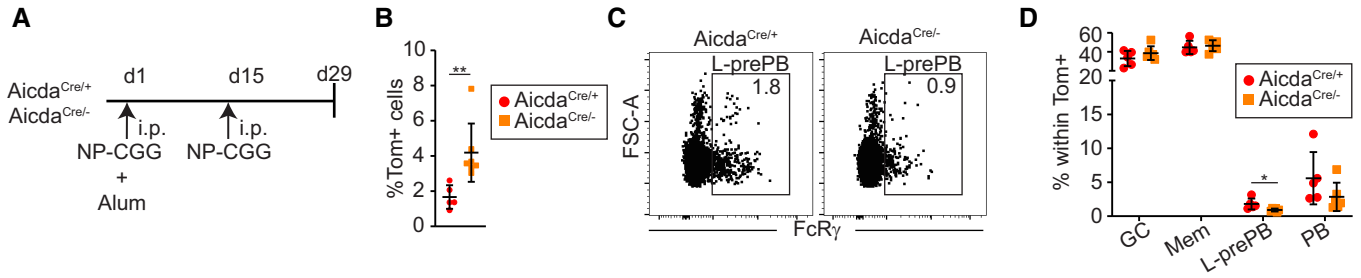

Figure EV4. L-prePB identification in NP-CGG immunized mice.

A Immunization protocol. Aicda$^{Cre/+}$ (n = 5) and Aicda$^{Cre/-}$ (n = 7) mice were immunized intraperitoneally (i.p.) with NP-CGG in alum. Two weeks later, mice were boosted with NP-CGG i.p.

B Quantification of spleen Tom$^+$ cells in NP-CGG immunized Aicda$^{Cre/+}$ (n = 5) and Aicda$^{Cre/-}$ (n = 7) mice.

C Representative flow cytometry plots of L-prePB staining (Tom$^+$ B220$^+$ CD138$^-$ GL7$^-$ FcRγ$^+$) in Aicda$^{Cre/+}$ and Aicda$^{Cre/-}$ mice.

D The proportion of GC B cells (B220$^+$ Tom$^+$ CD138$^-$ GL7$^+$), PB (Tom$^+$ CD138$^+$), Mem (Tom$^+$ B220$^+$ CD138$^-$ GL7$^-$ CD38$^+$ FcRγ$^-$), and L-prePB (Tom$^+$ B220$^+$ CD138$^-$ GL7$^-$ FcRγ$^+$) was determined by flow cytometry within total Tom$^+$ cells in Aicda$^{Cre/+}$ (n = 5) and Aicda$^{Cre/-}$ (n = 7) mice.

Data information: Bars and error bars indicate mean ± standard deviation. Statistics were calculated with an unpaired t-test. *$P \leq 0.05$, **$P < 0.01$.

Figure EV5. Comparative clonal analysis of Aicda$^{Cre/+}$ and Aicda$^{Cre/-}$ mice.

A Bar plot depicting the contribution of the different transcriptional clusters in expanded clones with more than 2 cells in Aicda$^{Cre/+}$ (top) and Aicda$^{Cre/-}$ (bottom) mice.

B UpSet plots showing quantification of clonal overlap between clusters identified in Fig 1D in Aicda$^{Cre/+}$ (left) and Aicda$^{Cre/-}$ (right). GC.LZ and GC.DZ populations were grouped and shown as GC for the sake of clarity.

C Cytoscape representation of all cluster interactions in Aicda$^{Cre/+}$ and Aicda$^{Cre/-}$ immune response, based on their clonal sharing probabilities. Red and orange connecting lines show the most increased cluster relationships in Aicda$^{Cre/+}$ and Aicda$^{Cre/-}$ mice, respectively.

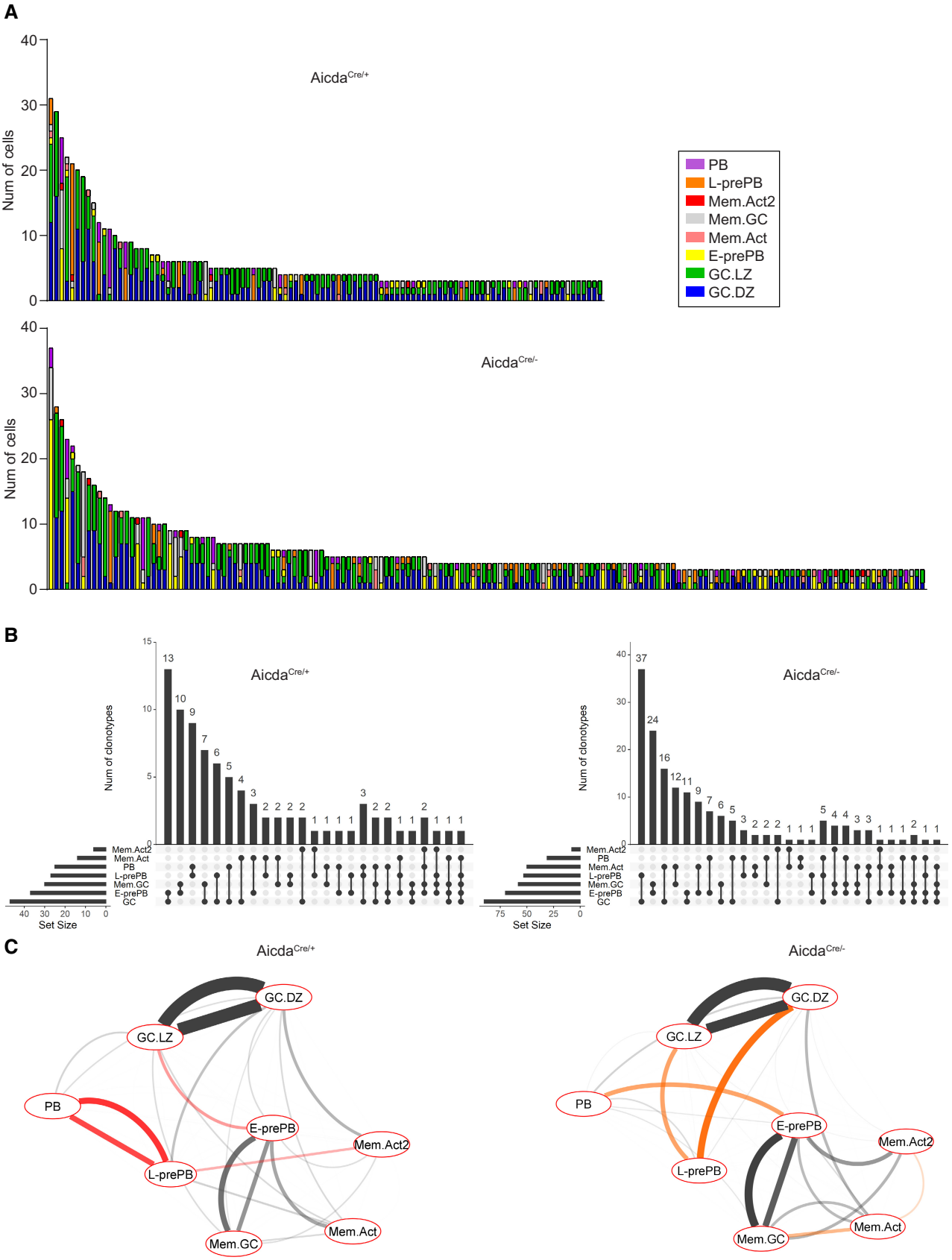
A
Aicda Cre/+
Aicda Cre/-
Num of cells
PB
L-prePB
Mem.Act2
Mem.GC
Mem.Act
E-prePB
GC.LZ
GC.DZ
B
Num of clonotypes
Set Size
C
GC.DZ
GC.LZ
PB
E-prePB
Mem.Act2
L-prePB
Mem.GC
Mem.Act

Figure EV5.